Coexistence of large amplitude stationary structures in a model of reaction-diffusion system

Andrzej L. Kawczyński and Bartłomiej Legawiec
Institute of Physical Chemistry, Polish Academy of Sciences, Kasprzaka 44/52, 01-224 Warsaw, Poland
(Received 5 May 2000; published 25 January 2001)

The two-variable reaction-diffusion model of a chemical system describing the spatiotemporal evolution to large amplitude stationary periodical structures in a one-dimensional open, continuous-flow, unstirred reactor is investigated. Numerical solutions show that the structures are generated by divisions of the traveling impulse and its stopping at the boundary of the system. Analyses of projections of numerical solutions on the phase plane of two variables elaborated in the present paper allow qualitative explanation of the results. The coexistence of the large amplitude stationary periodical structures is shown. A number of coexisting structures grows strongly with increasing length of the reactor and may be as large as one wishes. The relationship of these results to biological systems is stressed.

DOI: 10.1103/PhysRevE.63.021405 PACS number(s): 82.70.−y

I. INTRODUCTION

Since the pioneering work by Turing [1] it has become clear that minimal models that were able to describe the pattern formation in biological systems might be based on reaction-diffusion equations. This result stimulated searches of patterns in chemical systems [2]. In the 1970s so-called target patterns [3,4] and spiral waves [5,6] have been found in experiments performed in Petri dishes with thin layers of the Belousov–Zhabotinsky (BZ) reactions [4,7]. These patterns were transient ones, because the experiments were performed in closed chemical systems. Experimental studies of stationary (asymptotic) patterns require sustained far-from-equilibrium conditions [2]. Such conditions have been created in an open Couette reactor, which allows the strong increase of effective diffusion coefficients [8], but extensive laboratory studies begun in the 1980s when open, continuous-flow, unstirred reactors (CFUR) were constructed [9]. In CFURs patterns form inside a gel layer with well-defined reagent concentrations at its boundaries. In this way natural convection, which is caused by concentration (density) inhomogeneities, may be eliminated and the behavior of the system is determined by reaction and diffusion processes only. Sustained nonequilibrium conditions may be maintained indefinitely by a continuous refreshment of chemical reservoirs being in contact with the gel boundaries. Besides the BZ system, two others ones have been extensively studied, namely the chloride-iodide-malonic acid (CIMA) system [10] and the ferrocyanide-iodate-sulfite (FIS) reaction [11]. A kind of observed pattern depends on a geometry of the system and therefore CFURs with various geometries have been used in experiments. Thin-strip reactors [12,13], disk reactors [14,15], and also CFURs with other geometries have been used [16,17]. Patterns observed in one-dimensional reactors may be observed also in two- and three-dimensional ones but not vice versa. In the one-dimensional Couette reactor besides the traveling front, two kinds of single steady front, two, and three steady fronts, one, two and three oscillating fronts, simple and complex colliding fronts, bursting fronts, bursting and oscillating fronts, and alternating bursting and colliding fronts have been observed [8]. Experiments in two-dimensional CFURs have revealed spiral waves [18,19]; hexagonal, striped, and rhombic stationary, periodic Turing patterns [12–15,20–23]; repulsive fronts, lamellar structures, and self-replicating and oscillating spots [24,25].

Predictions and understanding of these experimental results is mainly based on the bifurcation theory. Amplitude equations derived from the perturbation method allow one to determine stability of assumed solutions. In this way the appearance of subcritical or supercritical Turing structures has been predicted, as the consequence of instability of homogeneous stationary or oscillating solutions due to infinitesimal spatial disturbances [1,2,26–29]. Analyses of the Ising–Bloch bifurcation [30], where a stationary front bifurcates into two counter propagating fronts in a bistable reaction-diffusion model, have suggested that this bifurcation is the crucial effect in formation of lamellar structures [31–34] and other patterns [35] observed in the CIMA system [24,25].

Modeling of real patterns is strongly hindered by the fact that all chemical systems in which such patterns have been observed are complex in the sense that many variables (concentrations of reagents) must be used in their models. To the best of our knowledge, there are no theorems which allow one to predict the formation of the patterns in two and more variables reaction-diffusion systems in one and more spatial dimensions. There are well-known theorems by Kanel [36,37], Fisher [38], and Kolmogorov, Petrovsky, and Piskunov [39], which define general properties of kinetic terms necessary and sufficient to obtain solutions in the form of traveling fronts, but these theorems concern reaction-diffusion systems with one variable only. Therefore modeling and predictions of the pattern formation are based mainly on numerical simulations of generic or specially selected models of reaction-diffusion systems. However, the Kanel theorem or the Fisher and Kolmogorov, Petrovsky, and Piskunov theorem can be helpful in analyses of models with many variables provided there is the possibility to separate different time scales for individual variables. This approach has been allowed to construct models of target patterns (leading center [40,41]), large amplitude stationary periodical structures [42–45], oscillating fronts (chemical pulsar [46,47]), bursting fronts (standing waves [48]), and modulated large amplitude stationary structures [49]. The other approach based on the construction of stationary structures in

two-variable (activator-inhibitor) systems in an excitable regime has also been elaborated [50–53].

In this paper we present studies of stationary periodical structures and therefore it is necessary to stress the difference between small amplitude stationary periodical Turing structures and large amplitude ones. The small amplitude stationary periodical structures are generated due to the Turing instability in which a homogeneous stationary state becomes unstable to spatial disturbances. The large amplitude stationary periodical structures are generated in excitable or bistable systems in which homogeneous stationary states remain stable to small disturbances and the structures may be generated provided disturbances are sufficiently large. Such structures may also appear in homogeneously oscillating systems by sufficiently large local disturbance [45]. There are two main routes of the generation of large amplitude stationary periodical structures in one-dimensional reaction-diffusion systems. One of them is the generation of new pulses of excitation before previously generated pulses [43]. The other one is the formation of the structures by division and the stopping of traveling impulses [44,45,54,55]. These effects have been used in modeling of stationary periodical structures in three-variable reaction-diffusion systems [42–45]. The third variable is important in these models because its spatial distribution controls bifurcations from excitable to bistable regimes. Recently, large amplitude stationary periodical structures as well as other patterns have been found in the two-variable reaction-diffusion model for periodic boundary conditions [54,55]. These structures have been observed in the Gray–Scott [56,57] model with three stationary states, one of them was a stable focus, whereas two others were unstable (a saddle-point and an unstable focus) with a sufficiently large difference in diffusion coefficients. They appear due to division and stopping of a traveling impulse. If the difference in diffusion coefficients is not large enough, then the well-known traveling impulse is observed. These results have been obtained by numerical solutions and their explanation is still open. Nevertheless, this is a very important observation, because it offers new possibilities in modeling of the patterns. Each pattern observed in the n variable model can be found in the $(n+1)$ variable model obtained by adding one variable. The $(n+1)$ variable model usually has more ample homogeneous dynamics and may exhibit a richer variety of spatiotemporal patterns than the n variable one.

In the present paper we describe the formation of large amplitude stationary periodical structures in a one-dimensional system described by two reaction-diffusion equations. We present also explanations of division and stopping of traveling impulses. Our analysis is based on qualitative estimations of reaction and diffusion terms in the kinetic equations on a phase plane corresponding to a homogeneous system. Like the Gray–Scott model our system has the same type of three stationary states (stable and unstable foci and a saddle-point). In the Gray–Scott model nullclines for corresponding ordinary differential equations are discontinuous and therefore the analysis of it is difficult. In our model the nullclines are continuous and the reaction-diffusion system is easier to analyze. Our model is based on the realistic scheme of elementary chemical reactions in which dynamics at reasonable assumptions may be reduced to two variables.

II. MODEL

The model consists of the following elementary, monomolecular, and bimolecular reactions (excluding autocatalysis):

$$S_0 \underset{k_{-1}}{\overset{k_1}{\rightleftharpoons}} S, \tag{1}$$

$$S + E \underset{k_{-2}}{\overset{k_2}{\rightleftharpoons}} SE, \tag{2}$$

$$SE \overset{k_3}{\rightarrow} E + P, \tag{3}$$

$$SE + S \underset{k_{-4}}{\overset{k_4}{\rightleftharpoons}} S_2E, \tag{4}$$

$$P + E \underset{k_{-5}}{\overset{k_5}{\rightleftharpoons}} EP, \tag{5}$$

$$P + SE \underset{k_{-5}}{\overset{k_5}{\rightleftharpoons}} SEP, \tag{6}$$

$$P + S_2E \underset{k_{-5}}{\overset{k_5}{\rightleftharpoons}} S_2EP, \tag{7}$$

$$P + E' \underset{k_{-6}}{\overset{k_6}{\rightleftharpoons}} E'P, \tag{8}$$

$$E'P \overset{k_7}{\rightarrow} E' + R, \tag{9}$$

$$P \overset{k_8}{\rightarrow} Q. \tag{10}$$

We assume that S_0 is a reservoir variable, whose concentration is maintained constant. Alternatively, steps (1) may

be treated as inflow/outflow terms in a continuously stirred tank reactor (CSTR). The reactant S is transformed to the product P with E as the catalyst [steps (2) and (3)]. This part of the scheme is the well-known Langmuir–Hinshelwood mechanism of a catalytic reaction (or the Michaelis–Menten kinetics for an enzymatic reaction). Step (4) is the inhibition of the Langmuir–Hinshelwood mechanism (or the Michaelis–Menten scheme) by an excess of the reactant *S*. The next three steps present an allosteric inhibition of free enzyme as well as its complexes with reactant by an excess of the product *P*. It is noteworthy that many enzymes are inhibited by their reactants and products. For simplicity we assume that rate constants in steps (5)–(7) are the same, which is a reasonable assumption for allosteric inhibition by the product. The product *P* is consumed by another enzymatic reaction with the enzyme E' producing inreactive product *R* [steps (8) and (9)] and moreover, *P* is transformed directly to some product *Q* in step (10). This second enzymatic reaction allows simplification of formulas for a nullcline for the product.

According to the mass action law, the behavior of the system is described by ten kinetic equations for *S*, *P*, *E*, *SE*, *EP*, S_2E, *SEP*, S_2EP, E', and SE', but it is easy to notice that $E(t)+SE(t)+EP(t)+S_2E(t)+S_2EP=E_0$ and $E'(t)+E'P(t)=E_0'(t)$ are constant, so the system has two first integrals. Therefore one of the variables: *E*, *SE*, *EP*, S_2E, *SEP*, or S_2EP and E' or SE' can be calculated if others are known and the dynamics of the system is described by eight kinetic equations only. Usually, total concentrations of the enzymes E_0 as well as E_0' are much smaller than the concentrations of the reactant *S* and the product *P*. In this case one can separate scales of time, in which the concentrations of the reagents change. The variables *E*, *SE*, *EP*, S_2E, *SEP*, S_2EP, and E' become fast variables, whereas *S* and *P* are the slow ones. According to the Tikhonov theorem [58], the fast variables in a slow time scale are equal to their quasistationary values and in this scale the dynamics can be described by a reduced system of slow variables. The kinetic equations for *S* and *P* in dimensionless form are

$$\frac{ds}{dt}=A_1-A_2s-\frac{s}{(1+s+A_3s^2)(1+p)}, \tag{11}$$

$$\frac{dp}{dt}=B\left(-\frac{B_1p}{K_m'+p}-B_2p+\frac{s}{(1+s+A_3s^2)(1+p)}\right), \tag{12}$$

where $s=[S]/K_m$ and $p=K_5[P]$, are dimensionless concentrations of *S* and *P*, respectively, and $\tau=(k_3[E_0]/K_m)t$ is dimensionless time. The parameters are defined as follows: $K_m=(k_{-2}+k_3)/k_2$, $K_m'=(k_{-6}+k_7)/k_6$, $K_5=k_5/k_{-5}$, $A_1=k_1[S_0]/k_3[E_0]$, $A_2=k_2K_m/k_3[E_0]$, $A_3=(k_4/k_{-4})K_m$, $B=K_mK_5$, $B_1=k_7[E_0']/k_3[E_0]K_5$, and $B_2=k_8/k_3[E_0]K_5$.

If K_m' is much smaller than *p* the term $B_1p/(K_m'+p)$ can be replaced by B_1 and the dynamics of *p* is described by

$$\frac{dp}{dt}=B\left(-B_1-B_2p+\frac{s}{(1+s+A_3s^2)(1+p)}\right). \tag{13}$$

Nullclines for *s* and *p* are given by

$$p=\frac{s}{(1+s+A_3s^2)(A_1-A_2s)}-1, \tag{14}$$

$$p=\frac{-(B_2+B_1)+\sqrt{(B_2+B_1)^2-4B_2[B_1-s/(1+s+A_3s^2)]}}{2B_2}, \tag{15}$$

respectively.

These formulas allow for a selection of the parameters which gives one or three intersection points of the nullclines. Two intersection points correspond to a saddle-node bifurcation. The intersection points correspond to stationary states for the homogeneous system.

We assume that the reactions (1)–(10) occur in an one-dimensional CFUR. Only the reactant *S* and product *P* are able to diffuse, whereas all other reagents are immobilized in an appropriate gel which also eliminates the natural convection. In this case the time-space behavior of the system is described by two kinetic equations in the form:

$$\frac{\partial s}{\partial t}-D_s\frac{\partial^2 s}{\partial x^2}=A_1-A_2s-\frac{s}{(1+s+A_3s^2)(1+p)}, \tag{16}$$

$$\frac{\partial p}{\partial t}-D_p\frac{\partial^2 p}{\partial x^2}=B\left(-B_1-B_2p+\frac{s}{(1+s+A_3s^2)(1+p)}\right), \tag{17}$$

where D_s and D_p are dimensionless diffusion coefficients and *x* is the dimensionless space coordinate. In the sequel we consider the initial-boundary value (Cauchy) problem with initial conditions: $s(0,x)=s_{in}$ and $p(0,x)=p_{in}$ in one or more subintervals of $[0,L]$, and $s(0,x)=s_I$ and $p(0,x)=p_I$ for the complement of $[0,L]$, and the zero-flux boundary conditions at $x=0$ and $x=L$.

III. NUMERICAL RESULTS

We assume the following values for the parameters: $A_1=10^{-2}$, $A_2=10^{-4}$, $A_3=0.505$, $B=0.625$, B_1

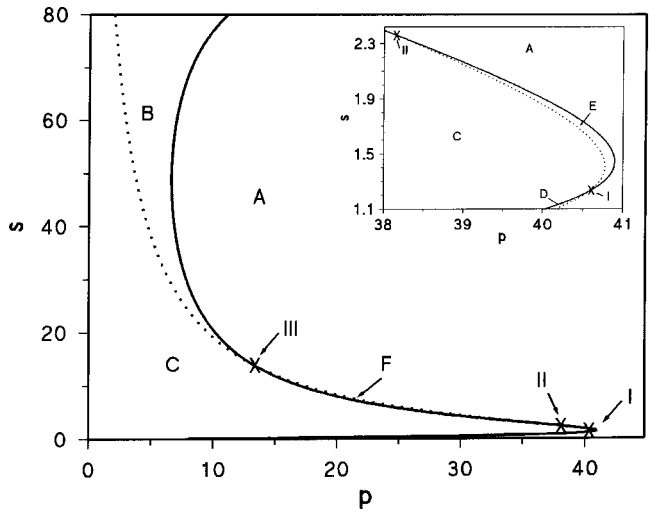

FIG. 1. Nullclines for s (continuous line) and for p (dotted line) on the phase plane (p,s). The regions with different signs of the vector fields for p and s are denoted by A, B, C, D, E, and F.

$=7.99\times10^{-3}$, $B_2=4.65\times10^{-5}$, $D_s=10^{-5}$, and $D_p=5\times10^{-5}$.

The nullcline for s on the phase plane (p,s) has an S-shape with three branches: the lower branch which is attracting, the repelling middle branch, and the attracting upper branch. The upper branch approaches asymptotically $s=A_1/A_2$ for p going to infinity.

For these values of the parameters Eqs. (11) and (13) have three stationary states:

$$s_I=1.227\,542\,47, \quad p_I=40.585\,927\,8, \tag{18}$$

$$s_{II}=2.362\,912\,366, \quad p_{II}=38.144\,272\,305, \tag{19}$$

$$s_{III}=13.885\,593\,25, \quad p_{III}=13.364\,314\,68. \tag{20}$$

The state I is a stable node, II is a saddle point, whereas III is an unstable focus.

The nullclines shown in Fig. 1 separate the phase plane (p,s) into six regions. In region A the kinetic term for s (s-component of vector field) is positive and the kinetic term for p (p-component of vector field) is negative. This means that in this region s increases and p decreases in the homogeneous system. In region B both kinetic terms are negative and the variables s and p decrease. In region C the kinetic term for s is negative and the kinetic term for p is positive which means that s decreases and p increases. In region D both components of the vector field are positive and s and p increase. In region E both kinetic terms are negative and therefore s as well as p decreases. In region F both components of the vector field are positive and s as well as p increase.

An evolution of the system strongly depends on a ratio of diffusion coefficients and on values of initial conditions. Of course, if initial disturbance of the stable stationary state I is sufficiently small, then the system will evolve to homogeneous distributions of s and p given by the state I. In order to obtain nontrivial evolutions in the form of the traveling impulse, the initial condition s_{in} should be higher than some critical value and an excited subinterval of x should be sufficiently large. For equal diffusion coefficients an evolution of sufficiently large initial disturbance is similar as for excitable systems with one stable stationary state. The single traveling impulse is formed and spreads through the system with constant velocity without changing its shape, and disappears at the boundaries. A completely different situation is observed if the ratio of diffusion coefficients D_p/D_s is sufficiently large. An example of the evolution for the following initial condition

$$s(0,x)=s_{in} \text{ for } x\in[0,l] \text{ and } s(0,x)=s_I \text{ for } x\in(l,L], \tag{21}$$

$$p(0,x)=p_{in} \text{ for } x\in[0,l] \text{ and } p(0,x)=p_I \text{ for } x\in(l,L] \tag{22}$$

(with $l\ll L$) is shown in Fig 2. In the sequel we describe in detail this evolution. The initial profile becomes continuous due to diffusion and the maximal value of s in disturbed interval grows whereas p decreases. The neighborhood positioned to the right of l is subsequently excited and the front of excitation is formed [see Fig. 2(a), continuous line]. Simultaneously a local minimum of s is formed before the front of excitation. Next, at $x=0$ and inside l s falls down and p grows [see Figs. 2(a) and 2(d), long dashed lines] which follows in formation of the first impulse [see Figs. 2(a) and 2(d), dashed lines]. This impulse is traveling to the right but its shape changes [compare dashed lines with dotted lines in Figs. 2(a) and 2(d)]. When the impulse approaches a vicinity of the right boundary it slows down and stops. In sufficiently long systems the first impulse divides spontaneously creating new pulses behind it, as is shown in Figs. 2(b) and 2(e) and 2(c) and 2(f). New pulses do not divide themselves but their shapes evolve slowly approaching stationary distributions during long periods of time [see Figs. 2(b), 2(e), 2(c), and 2(f)]. The division is stopped when the first impulse approaches the vicinity of the right boundary. In a spatially infinite system the division of the first impulse will be continued up to infinity.

Of course, transient solutions depend on initial conditions which is a typical property for partial differential equations of the parabolic type, but in our model also asymptotic, stationary solutions exhibit such dependence. This means that different stationary structures may coexist in the same system. An example of such coexistence is shown in Figs. 3(a) and 3(b), where only four among ten possible different patterns are shown. The pattern with two pulses inside and the half of the pulse at the left boundary and its symmetric reflection, and the pattern with one pulse inside and the half at the right boundary as well as three patterns with two halves of the pulse at both boundaries are not shown in this figure. Any stationary periodical structure exists in some interval of L. At a minimal interval L a pattern consists of some number of pulses with single maximum for large values of s and small maximum at low values of s. If the size of the system grows the single maximum at large s initially increases but at some size it starts to decrease and with further growth of L it splits into two maxima and minimum between them. The

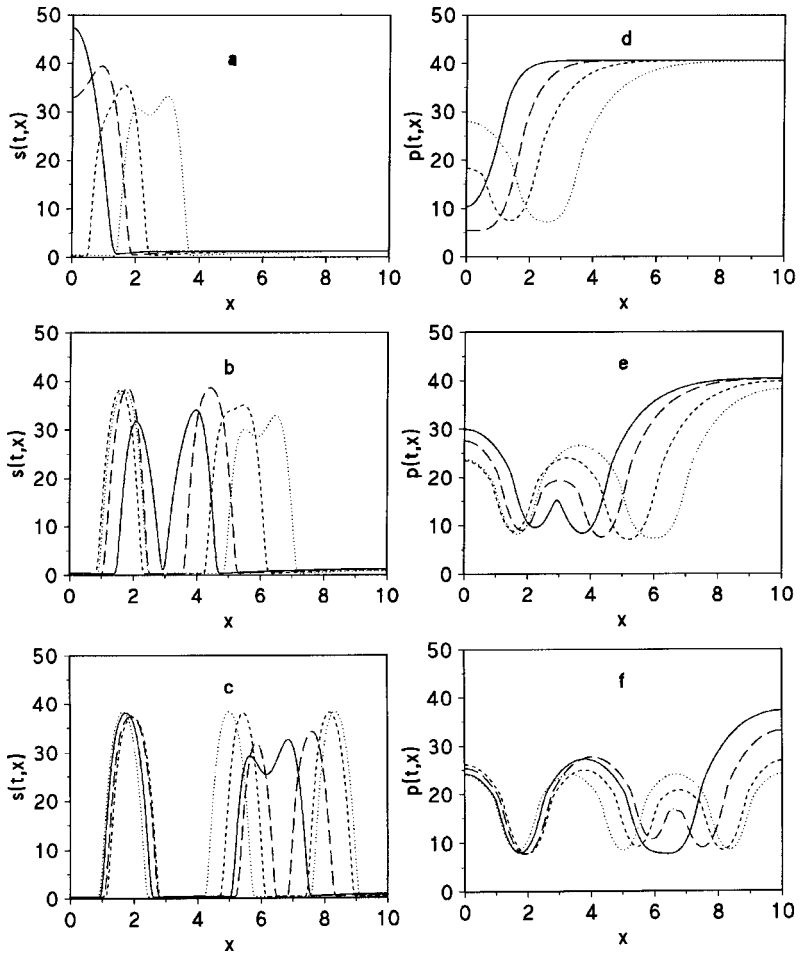

FIG. 2. Spatiotemporal evolution of $s(t,x)$ (a,b,c) and $p(t,x)$ (d,e,f) on the interval [0,10] for the following initial conditions: $s(0,x)=20$ for $x\in[0,0.1]$ and $s(0,x)=s_I$ for $x\in(0.1,10]$; $p(0,x)=35$ for $x\in[0,0.1]$ and $p(0,x)=p_I$ for $x\in(0.1,10]$; and the boundary conditions $(\partial s/\partial x)|_0=(\partial s/\partial x)|_1=(\partial p/\partial x)|_0=(\partial p/\partial x)|_1=0$. (a) and (d): continuous lines, $t=12\,500$; long dashed lines, $t=25\,000$; dashed lines, $t=50\,000$; and dotted lines, $t=150\,000$; (b) and (e): continuous lines, $t=235\,000$; long dashed lines, $t=275\,000$; dashed lines, $t=350\,000$; and dotted lines, $t=412\,500$. (c) and (f): continuous lines, $t=475\,000$; long dashed lines, $t=557\,500$; dashed lines, $t=625\,000$; and dotted lines, $t=2\,500\,000$.

maximum at small values of s increases in the whole region of L where the stationary structure exists.

It is easy to check that nonlinear, partial differential equations of the type considered here are symmetrical with respect to reflections in x. The consequence of this symmetry and the zero-flux boundary conditions is that patterns consisting of a given pattern and its reflections are also solutions of the system provided the selected pattern is the solution. In Fig. 4 the dependence of numbers of pulses in stationary periodical structures on size of the system is shown. Circles show minimal intervals on which a given pattern may exist, whereas triangles mark maximal intervals. These points lie along two straight lines, which is the consequence of the symmetry of the system. The lines are described by

$$y_{\min}=0.6250\cdot L, \tag{23}$$

$$y_{\max}=0.1895\cdot L \tag{24}$$

and the maximal and minimal number of pulses in a stationary periodical structure for a given L are determined by

$$n_{\max}=[0.6250\cdot L]_{\max}, \tag{25}$$

$$n_{\min}=[0.1895\cdot L]_{\min} \tag{26}$$

where the symbols $[\cdot]_{\max}$ and $[\cdot]_{\min}$ denote a nearest less number and a nearest greater number of the type $1/2\cdot n$ for $n=0,1,\ldots$, respectively.

The stationary structures obtained in our model may consist of integer pulses or have additionally a half of a pulse at one or both boundaries. Therefore for a given L a number of coexisting stationary periodical structures is given by

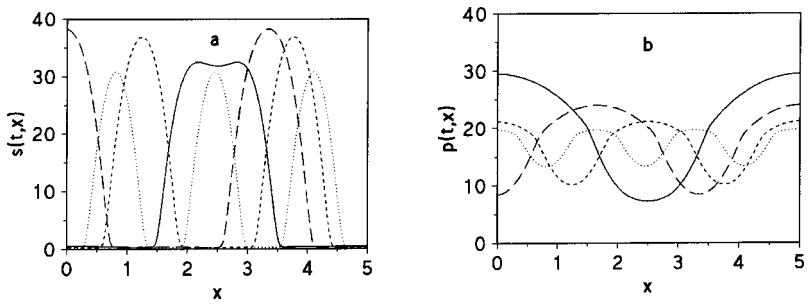

FIG. 3. Examples of the stationary periodical structures coexisting on the interval $L=5$: continuous lines, one pulse; long dashed lines, one and a half pulse; dashed lines, two pulses; and dotted lines; three pulses. The structure with two and a half pulses existing on this interval is not shown.

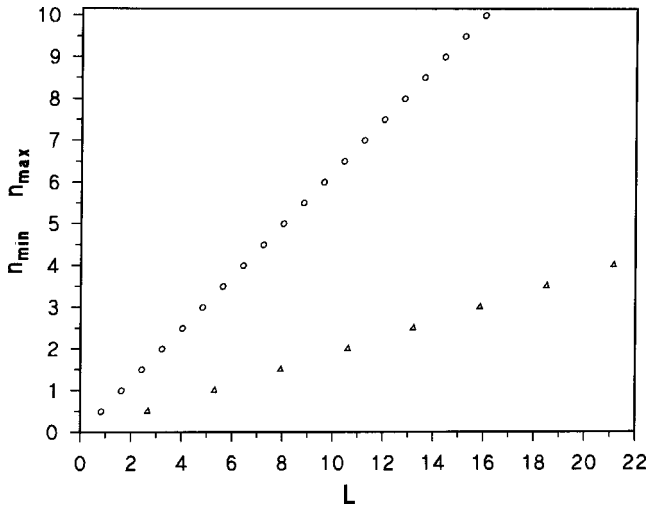

FIG. 4. Dependence of numbers of pulses in stationary periodical structures on a size (L) of the system. Circles denote the minimal L on which patterns with a given number of pulses may exist. Triangles mark the maximal L on which patterns with a given number of pulses may exist.

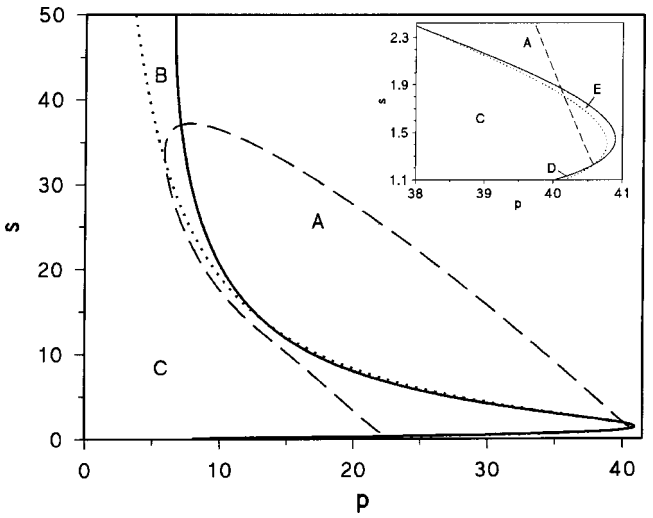

FIG. 5. Projection of $p(t,x)$ and $s(t,x)$ forming the stationary traveling impulse on the phase plane (p,s) for equal diffusion coefficients $D_p=D_s=10^{-5}$. Thick continuous line denotes the nullcline for s, thick dotted line the nullcline for p.

$$N=2[2(n_{\min}-n_{\max})+1]. \tag{27}$$

This number strongly increases with L.

IV. QUALITATIVE ANALYSIS

In the theory of ordinary differential equations a projection of states of a system on its phase space is a fundamental tool [59]. In the phase space solutions of the system are represented by trajectories in which exact information about time dependence of the solutions is lost.

States of a system described by partial differential equations of the parabolic type may by analyzed in similar way, but in this case the phase space corresponds to continuous distributions in space of the variables and has infinite uncountable dimension. Therefore such an approach is practically unprofitable. However, some qualitative information may be extracted from the projection of solutions to the partial differential equations on the phase space for ordinary differential equations in which diffusion terms are omitted. In this approach, exact information about the dependence of variables on space and time is lost, but changes in shapes of obtained projections allows one to explain and predict qualitative properties of spatiotemporal evolution of the system. In the sequel we will use this approach in the qualitative analysis of solutions $s(t,x)$ and $p(t,x)$ to Eqs. (16) and (17) by projections of them on the phase plane (p,s). For the ordinary differential equations (11) and (13) a state of the system is identified with a point in the phase plane (p,s). In our approach a projection of the solutions $s(t,x)$ and $p(t,x)$ to the partial differential equations (16) and (17) corresponds to a curve in the phase plane (p,s). A solution to Eqs. (11) and (13) gives a phase trajectory, which is the curve on the phase plane (p,s), whereas an evolution described by Eqs. (16) and (17) gives continuous transformations of a given curve into other curves on the same plane. Let us mention that stationary homogeneous solutions $s(t,x)$ and $p(t,x)$ correspond to points on (p,s), because in this particular case there is no difference between the partial and the ordinary equations. Solutions $s(t,x)$ and $p(t,x)$ in the form of a stationary traveling impulse, which spreads in infinite system (initial value problem), give on the phase plane (p,s) an invariant curve which starts and ends at the stable stationary state I. Sufficiently far from the front of the impulse and behind the back of it, $s(t,x)$ and $p(t,x)$ are very close to the stable stationary state I. The solution in the form of the stationary traveling impulse is obtained for Eqs. (16) and (17) in the case of equal diffusion coefficients. In this case the curve crosses in turn the following regions: C, E, A, B, C, and D (see Fig. 5). For finite systems the closed curve is only an approximation which is reasonable, if the front and the back of the impulse are far from boundaries of a system. It is noteworthy that the same sequence of crossed regions, excluding the regions C and E, is obtained in the homogeneous system for a trajectory starting from the region A above the middle branch of the nullcline for s.

If the ratio of the diffusion coefficients is sufficiently large, then the impulse changes its shape when traveling, and its projection on the phase plane (p,s) will be a curve, but its contour will change. The qualitative analysis described below allows us to determine the form of the projection which corresponds to asymptotic solutions of the Eqs. (16) and (17). Our analysis of the solutions to Eqs. (16) and (17) is based on estimations of reaction and diffusion terms at extreme values of p and s and in their close neighborhoods. We will concentrate our analysis on the evolution of projections for the initial conditions (21) and (22).

In the initial interval of time the front of the impulse is formed (see Fig. 6, continuous line) and projections of the profiles of $s(t,x)$ and $p(t,x)$ on the phase plane form the curve which starts at the stable stationary state I at $x=L$ (the right tip), where s has initially its local minimum and p reaches maximum, and ends at the maximum value of s and

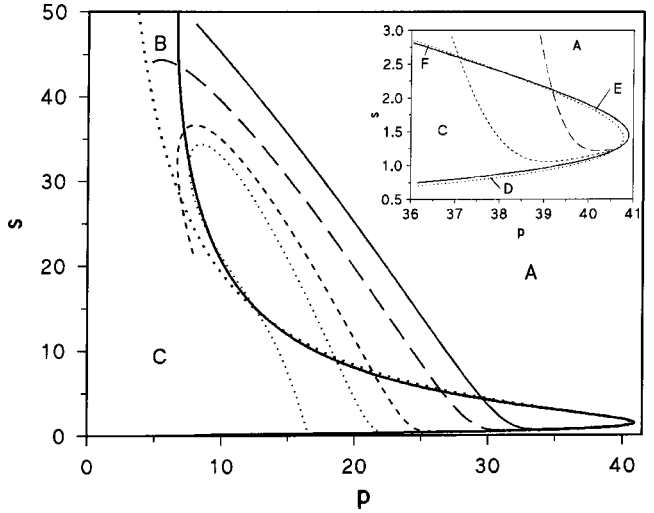

FIG. 6. Projections of $p(t,x)$ and $s(t,x)$ on the phase plane (p,s) at selected times showing the formation of the first impulse on the interval with $L=3$. Continuous line, $t=14\,000$; long dashed line, $t=19\,000$; dashed line, $t=33\,000$; and dotted line, $t=44\,000$. Inset shows the formation of a minimum of $s(t,x)$ before the front of the first impulse. Long dashed line, $t=500$ and short dashed line, $t=2000$. Thick continuous line denotes the nullcline for *s*, thick dotted line the nullcline for p.

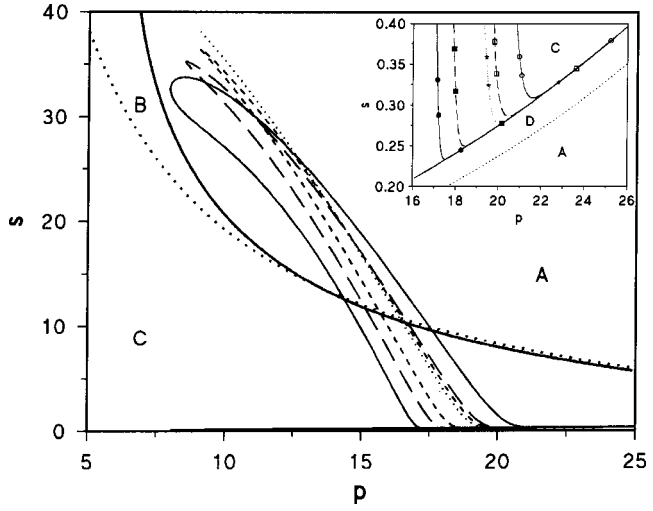

FIG. 7. Continuation of the projection's evolution shown in Fig. 6. The evolution of the projections to stationary one pulse structure is shown for the following times: continuous line, $t=50\,000$; long dashed line, $t=60\,000$; dashed line, $t=68\,000$; and dotted line, $t=1\,500\,000$. Inset shows the decrease of p at $x=L$ in time. Continuous line with open circles, $t=50\,000$; long dashed line with open squares, $t=60\,000$; and dotted line with stars, $t=1\,500\,000$. The left most symbols denote values of p at $x=L$. The increase of values of p at $x=0$ for the same times is shown by the same solid symbols. Thick continuous line denotes the nullcline for *s*, thick dotted line the nullcline for p.

the minimum value of p at $x=0$ (the left tip). Due to the condition $D_p>D_s$, the piece of the curve starting at the right tip, which lies between the lower and the middle branches of the nullcline for *s*, is shifted to left, as compared with the equal diffusion coefficients case, and is pushed out from the region *E* to the regions *C* and *F*, because the negative value of the diffusion term for *p* prevails over its kinetic term. Moreover, because *s* is a faster variable as compared with *p*, the negative kinetic term for *s* prevails over its positive diffusion term and the piece of the curve is shifted down close to the lower branch of the nullcline for *s* (see the inset in Fig. 6). In this way a small local minimum of *s* before the front of the impulse is formed. The whole projection appears to be in regions *C*, *F*, and *A*. The left tip of this curve is in the region *A* where the kinetic term for *s* is positive, but its diffusion term is negative and the kinetic term for *p* is negative, whereas its diffusion term is positive. In this interval of time both kinetic terms at the left tip prevail over the diffusion terms and in consequence, the left tip moves upwards and left on the phase plane. At some moment of time the left tip approaches the nullcline for *s*. After crossing of this nullcline the tip appears to be in region *B* where both kinetic terms are negative. The negative kinetic term for *s* is amplified by the negative diffusion term and *s* at the left tip decreases more quickly than in its surroundings. In consequence, at some moment of time instead of the local maximum of *s* at $x=0$ the local minimum of *s* is formed (see Fig. 6, long dashed line). The diffusion term for *s* changes its sign from negative to positive but its value is to small to stop the decreasing of $s(t,0)$. The minimum of *s* becomes deeper and at some time the tip crosses the nullcline for *p*. After crossing this nullcline the left tip appears to be in region *C* where the kinetic term for *p* is positive, so $p(t,0)$ starts to grow forming a local maximum which is accompanied by a change of the sign of its diffusion term from positive to negative (see Fig. 6, dashed line). At the left tip $s(t,0)$ falls down close to a vicinity of the lower branch of the nullcline for *s* and simultaneously $p(t,0)$ continues its growth. In this way the back of the impulse is formed. The left tip shifts itself inside the region *C* very close to the lower branch of the nullcline for *s* and tends slowly to the stable stationary state *I* because the diffusion term is to small to stop the increase of *p*. In this way the first impulse is created in the form of a loop consisting of the front (the part of the projection positioned to the right from the maximum for *s*) and the back (the part positioned to the left from the maximum for *s*) (see Fig. 6, dotted line). Simultaneously, in region *B* on the piece of the back positioned between the nullclines a local minimum of *p* is formed. The diffusion term for *p* is positive and prevails over the kinetic term. Therefore this piece of the projection is shifted to the right and next pushed out from region *B* to regions *A* and *F* (compare the dotted line in Fig. 6 with the continuous line in Fig. 7). The projection of the impulse extends from the right tip ($x=L$) which is close to the stable stationary state *I* and goes through *C*, *F* to the maximum of *s* positioned in *A* (the front of the impulse) and from the maximum of *s* through *A*, *F*, and *C*, and ends at the left tip ($x=0$) (the back of the impulse). Further evolution depends on the size of the system (compare Fig. 7 with Figs. 8 and 9). If the size is small ($L\approx 3$), then the small minimum of *s* before the front of the impulse attains a close neighborhood of the right boundary. At $x=L$ the second derivative of $p(t,x)$ with respect to x is negative and decreases while the front ap-

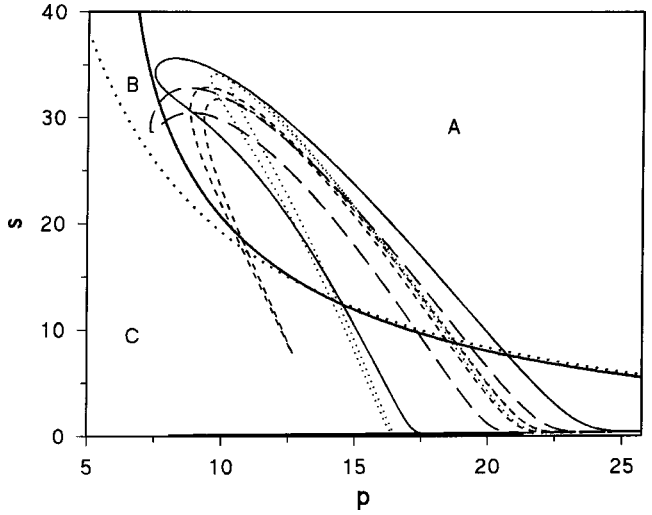

FIG. 8. Projections of $p(t,x)$ and $s(t,x)$ on the phase plane (p,s) at selected times showing the division of the first impulse on the interval with $L=6$. Previous evolution is very similar to that shown in Fig. 6. Continuous line, $t=54\,000$; long dashed line, $t=160\,000$; dashed line, $t=254\,000$; and dotted line, $t=260\,000$. The formation of the nose and its tip, as well as the pulse behind the first impulse is clearly seen. Thick continuous line denotes the nullcline for s, thick dotted line the nullcline for p.

proaches the right boundary. In consequence, $p(t,L)$ decreases because the kinetic term for it is very small here and the diffusion term prevails on it (see the inset in Fig. 7). Simultaneously, the second derivative of $s(t,x)$ at $x=L$ becomes more negative while the front approaches $x=L$. In consequence, the small local maximum of $s(t,L)$ decreases. This corresponds to a displacement of the right tip away

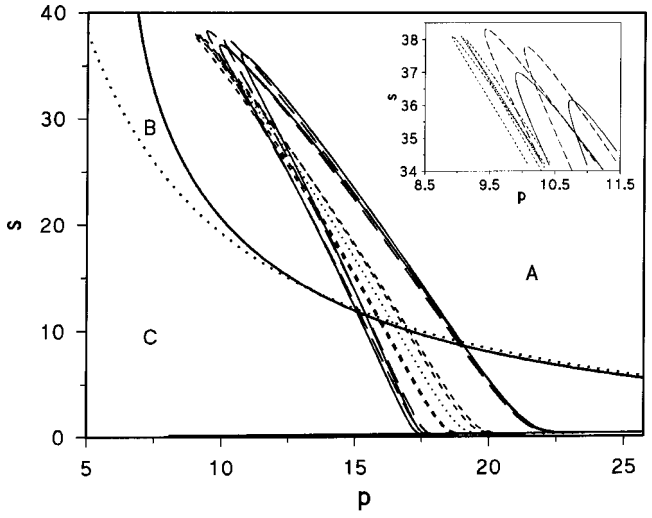

FIG. 9. The same as in Fig. 8 but here the evolution of the first impulse and the new pulse to asymptotic projection is shown for the following times: continuous line, $t=270\,000$; long dashed line, $t=280\,000$; dashed line, $t=340\,000$; and dotted line, $t=2\,000\,000$. Inset shows the details of the projections. The drift of the first impulse and the new pulse to the stationary structure is seen. Thick continuous line denotes the nullcline for s, thick dotted line the nullcline for p.

from the stable stationary state I along the lower branch of the nullcline for s (see the inset in Fig. 7). This displacement causes a threshold for excitation of the system from the state I that increases, and if the displacement is sufficiently large, then the front stops to move to the right. Next, slow changes of the whole projection occur. During this slow evolution the competition between diffusion and kinetic terms causes the loop formed by the front and the back of the impulse to become more and more narrow. Changes of the front and the back in regions A and C play an important role in this evolution. The narrowing of the loop may be explained in the following way.

For the part of the projection positioned in the region A the kinetic terms for p for the front and the back are negative. The kinetic term for the front is more negative than for the back, because a part of the projection corresponding to the back is closer to the nullcline for p than a part corresponding to the front. Moreover, the diffusion term for p attains its positive maximum at the minimum of p which is positioned in the back. Therefore at the minimum of p and around it the kinetic and the diffusion terms for p can compensate themselves much more exactly than in the front. The positive diffusion term for p can prevail over the negative kinetic term in the back, whereas the opposite condition is fulfilled in the front. Simultaneously, the kinetic and diffusion terms for s influence the part of the front and the back positioned in A. The positive kinetic terms for s attempt to shift the front as well as the back upwards but this movement is restrained by the negative diffusion term around the maximum of s. The diffusion term along the back has smaller absolute value than along the front and therefore a distance between them in the s direction decreases. At the maximum of s the diffusion term decreases and compensates the kinetic term more and more exactly. In consequence, the compensation of the kinetic terms with the diffusion terms for both variables leads to the joining of the front and the back.

In region C the kinetic term for p is positive and sufficiently large to prevail over the diffusion term along the back and the negative kinetic term for s is to small to compensate the positive diffusion term and therefore the projection of the back moves right and upwards. The front is positioned in a weaker vector field for p than the back. Let us mention that $p(t,x)$ at $x=L$ remains closer to p_I than at $x=0$ (see the inset in Fig. 7) and the minimum of p is positioned around the center of the system. Therefore at the front the diffusion term for p is more negative than at the back. The negative diffusion term prevails over the positive kinetic term and therefore the front moves to the left. On the other hand the diffusion term for s is positive but is to small to compensate the negative kinetic term. Therefore the projection of the front moves left and downwards and the distance between the front and the back decreases and they joint themselves asymptotically. In this way the loop consisting of the front and the back shrinks to ''single curve'' and the asymptotic distributions of both variables become symmetric with respect to the spatial center of the system.

If the size of the system is sufficiently large ($L\approx 6$ and larger, see Fig. 4), then the evolution is very similar to that presented in Fig. 6 and does not stop on the stationary first

impulse (Fig. 7) but continues in a different way (see Fig. 8). In such a case, the first impulse continues its traveling to the right boundary and the most important changes occur in the part of the projection positioned around the maximal value of s and the minimal value of p. This part is in the region A, where the vector field is positive for s and negative for p and the diffusion terms are negative and positive, respectively. The maximum of s starts to grow shifting this part of the curve to the region with a stronger field for p (compare continuous lines in Figs. 7 and 8). The kinetic term for p prevails over the diffusion term and in consequence a minimum of p in the back moves up and left, and at some moment has to cross the nullcline for s. After crossing the nullcline, a down oriented nose with the tip is formed (see Fig. 8, long dashed line). Formation of the tip of the nose corresponds to the appearance of the local minimum of s surrounded by two local maxima. The diffusion term for s becomes positive at the tip of the nose, but is to small to compensate the negative vector direction field for s and the tip of the nose moves down away from the nullcline for s approaching the nullcline for p at some moment of time. From this moment p at the tip of the nose starts to grow forming its local maximum (see Fig. 8, dashed line), but s decreases very quickly because of the very strong vector field for it and approaches values close to the lower branch of the nullcline for s. The tip of the nose moves in region C along the lower branch of the nullcline for s towards the stable stationary state I and the nose itself becomes very narrow. In this way the division of the first impulse occurs and a new pulse is formed behind it (see the dotted line in Fig. 8). The curve in the form of two loops is formed on the phase plane. The higher part of the whole projection corresponds to the first impulse, whereas the lower one corresponds to the newly created pulse. The first impulse consists of the front and the back and continues its traveling to the right boundary. The front of it starts at the right tip of the whole projection (at $x=L$) and ends at the maximum value of s whereas the back starts at the maximum value of s and ends at the tip of the nose. The newly created pulse does not change much its position in x. The part of the distribution in x positioned to the right from its maximum value of s corresponds to the left part of the projection on the phase plane (p,s) starting from the tip of the nose and ending at the maximum of s. The part of the profile in x positioned to the left from the local maximum of s corresponds to the right part of the projection, which starts at its maximum of s and ends at the left tip (at $x=0$) of the whole projection.

While the division of the first impulse develops, first the left part of the projection of the pulse is pushed out from region B, because in this region the diffusion term for p is positive and prevails over the negative kinetic term. Next, the projection of the back of the first impulse is also pushed out from region B for the same reason (see Fig. 8, dotted line). In the piece of the projection of the pulse around the maximum of s and the minimum of p the positive diffusion term for p is sufficiently large to shift this piece to the right. Simultaneously, this piece moves upwards, because the negative diffusion term for s is unable to compensate the positive kinetic term. The piece of the projection of the first impulse positioned around the maximum of s and the minimum of p moves upwards too, because the positive kinetic term for s prevails over the negative diffusion term for s (compare the dotted line in Fig. 8 with the continuous line in Fig. 9).

During further evolution both parts the pulse as well as the front and the back of the first impulse move upwards and approach each other, because the left parts of them remain in the weaker vector field for p than the right parts (see Fig. 9). The pieces close to the maximum of s and the minimum of p move to the left because they are shifted to the stronger vector field for p, where the kinetic term prevails over the diffusion term. The diffusion terms compensate the kinetic terms more and more accurately and asymptotically both parts of the pulse join. The evolution of the pulse is similar to the evolution of the first impulse shown in Fig. 7. Simultaneously, the projection of the front of the first impulse joins with its back and the loop corresponding to them joins with the loop for the pulse forming the ''single'' curve.

If a size of the system is larger, then after the formation of one pulse the evolution of the projection of the first impulse repeats the scenario described above and next the division of the first impulse may occur provided there is enough place in x before it (see Fig. 2). In this way subsequent new pulses may be generated in the system due to the division of the first impulse. If the first impulse attains the right boundary then it stops, because the threshold for excitation from the stable stationary state I increases. As it is explained above the increasing of the threshold is caused by the shift of the right tip away from the state I along the lower branch of the nullcline for s. After stopping, the first impulse evolves similarly to the pulses generated behind it and the piece of the projection of it attains the projections of the previous pulses. The tips of subsequent noses as well as the left tip corresponding to $x=0$ asymptotically attain the right tip and a stationary periodical structure is formed. Any stationary periodical structure has the projection in the form of a single curve along which the profiles of s and p are distributed a given number of times corresponding to a number of spatial periods composing the structure. This form of the projection on the phase plane differs substantially from the projection of the stationary traveling impulse observed at equal diffusion coefficients as well as from the projection of asymptotic oscillatory solutions to the ordinary differential equations, which are represented by closed curves.

The above analysis concerns initial conditions with disturbances of a small interval of x at the left boundary. For other initial conditions a spatiotemporal evolution is essentially the same. If the system is excited in some number of intervals of x, which are sufficiently separated, then excitations spread to both sides of disturbed intervals forming fronts. These fronts of excitation stop before they meet due to the same reasons as the front of the first impulse stops at the right boundary. Behind the fronts the backs of impulses are formed. If there is enough space in x, then each impulse leaves noses behind it according to the scenario described above for the first impulse. If initial conditions generate stationary periodical structures with half of the pulse at the right or the left boundary or at both of them, then in the evolution its part corresponding to the formation of the last nose is omitted. Instead

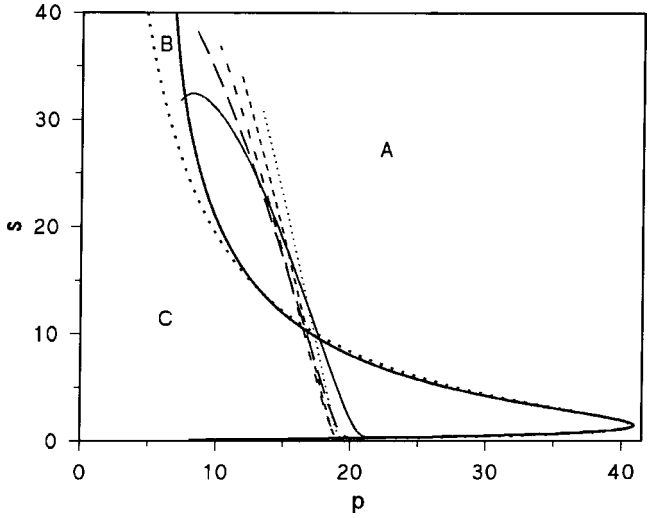

FIG. 10. Projections of $p(t,x)$ and $s(t,x)$ on the phase plane (p,s) for all stationary periodical structures coexisting on the interval $L=5$. One pulse structures, continuous line; one and a half pulse structures, long dashed line; two pulses structures, dashed line; two and a half pulses structures, short dashed line and three pulses structures, dotted line. Thick continuous line denotes the nullcline for s, thick dotted line the nullcline for p.

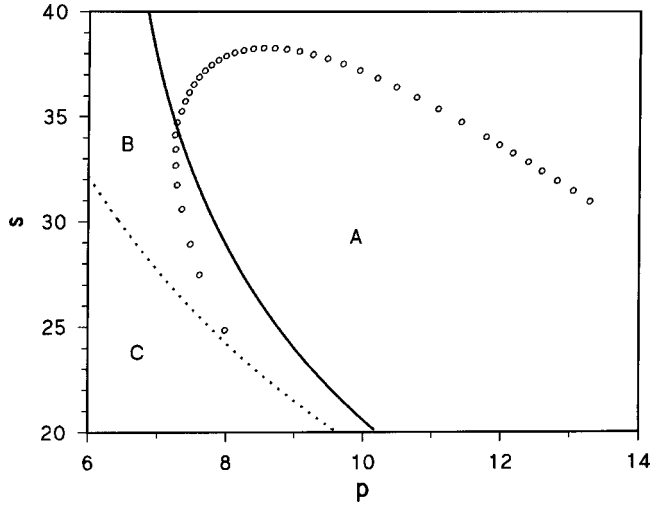

FIG. 11. Changes of the minimal values of p and extreme values of s for various sizes of the system. The left most and lowest symbol corresponds to all structures existing on maximal intervals of x, whereas the right most one denotes all structures existing on the minimal intervals of x. Thick continuous line denotes the nullcline for s, thick dotted line the nullcline for p.

of the formation of the last nose, the left or the right tip stops at the minimal value of p and maximal values of s.

Some number of stationary periodical structures may coexist for a given size of the system. Their projections on the phase plane (p,s) for $L=5$ are shown in Fig. 10. Each projection starts at the right tip positioned in region C very close to the lower branch of the nullcline for s in some distance from the state I, goes through the minimum value of s and next leaves region C, crosses the region F, and next goes through region A reaching the maximum value of s (see Fig. 10, dotted, short dashed, dashed, and long dashed lines) or eventually ends in region B reaching the local minimum of s positioned between two the maxima (see Fig. 10, continuous line). The stationary projections form a one parameter family of curves on the phase plane (p,s). In cases when a given structure exists at the maximal interval of x the projection of it cannot be described as a function $s=p(s)$ or adverse one and therefore the whole family cannot be described by a simple formula.

There exists a well-defined range in the phase plane (p,s) which is occupied by all stationary structures. In this range the kinetic terms are exactly compensated by the diffusion terms. This range may be characterized by the minimal and maximal values of p for a given size of the system. In Fig. 11 the circles denote the minimal values of p and extreme values of s. All symbols situated to the right of the nullcline for s correspond to the maximum values of s, whereas the symbols to the left of this nullcline correspond to the minimal values of s lying between two maxima of s. The left most and lowest symbol corresponds to all structures existing on maximal intervals of x, whereas the most right one denotes all structures existing on the minimal intervals of x. In Fig. 12 the stars denote the values of p and s at the boundaries, if structures consist of integer pulses. For structures with a half pulse the symbol denotes the maximum value of p and the maximum value of s situated in a range of small values of s for a given size of the system. These points lie very close to the nullcline for s, which means that diffusion terms for s are very close but not equal to zero. The right most point corresponds to all structures existing on the maximal intervals of x, whereas the left most one represents all structures existing on the minimal intervals of x.

V. DISCUSSION

In our model the stationary periodical structures appear due to two main effects: the division of the traveling impulse

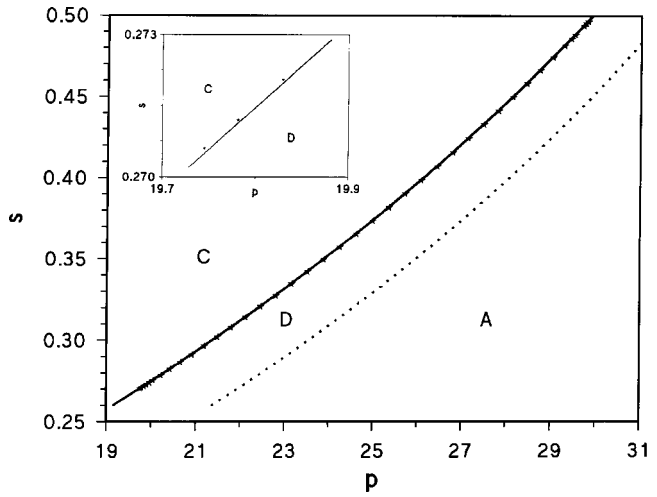

FIG. 12. Changes of the maximal values of p and maximal values of s for various sizes of the system. The right most symbol corresponds to all structures existing on the maximal intervals of x, whereas the left most one represents all structures existing on the minimal intervals of x. Thick continuous line denotes the nullcline for s, thick dotted line the nullcline for p.

and the stopping of its front at the boundary or at the meeting of two fronts spreading in opposite directions. Similar effects have been observed in other models of stationary periodical structures but they were caused by bifurcations from excitable to trigger regimes in a two-variable subsystem controlled by spatial distribution of the third variable [44,60]. The division of the traveling impulse in the present model is caused by the fact that the diffusion term for p is sufficiently large to shift a part of the projection of p and s on the phase plane (p,s) from region A, where the kinetic term for s is positive to region B, where this kinetic term is negative and sufficiently large to generate the nose which approaches a vicinity of the lower branch of the nullcline for s. The stopping of the front is caused by the fact that the diffusion term for p is sufficiently large to shift part of the projection of p and s away from the stable stationary state I in such a way that the distance from it to the middle part of the nullcline for s increases what stops the spreading of excitation of s. The analysis presented above allows one to explain in a qualitative way the results obtained in numerical calculations by showing whether reaction or diffusion terms prevail locally in Eqs. (16) and (17) what governs increasing or decreasing of the variables. The approach used in our analysis seems to be fruitful and may be applied to a qualitative analysis of other models. However, the analysis will be much more difficult for more than two variable models like the Oregonator [61] or the four-variable model for the FIS reaction [24], in which a large amplitude stationary structure as well as other patterns have been found in numerical calculations.

The coexistence of small amplitude stationary periodical structures has been found close to the Turing instability [62]. Spatial multistabilty of other patterns has also been discussed for a two-variable reaction diffusion model [63,64], but to our best knowledge, our model is the first example of the coexistence of the large amplitude stationary periodical structures in one-dimensional systems. A number of coexisting structures may be as large as one wishes, if the size of the system is sufficiently large. One can expect that in more dimensional systems different initial conditions may generate a very rich variety of observed patterns. The dependence of asymptotic patterns on initial conditions leading to their coexistence may also be helpful in the explanation of the diversity of patterns observed in physical systems like semiconductors [65] and premixed flames [66–68], which seem to be very important to biological systems [69].

The chemical scheme (1)–(10) is realistic because it is based on elementary monomolecular or bimolecular reactions excluding autocatalysis. The scheme contains some hints to look for such as kinetics in real chemical systems. It is well-known that many enzymes are inhibited by their reactants and products and therefore our model in two and/or three spatial dimensions seems to be helpful in the explanation of pattern formation in biological systems.

We believe that analogical evolutions may be observed in a two-variable generic system with similar shapes of the nullclines, in which the kinetic terms are replaced by cubic polynomial in the equation for s and linear terms in the equation for p.

[1] A.M. Turing, Philos. Trans. R. Soc. London, Ser. B **327**, 37 (1952).

[2] G. Nicolis and I. Prigogine, *Self Organization in Chemical Systems* (Wiley, New York, 1977).

[3] A.N. Zaikin and A.M. Zhabotinsky, Nature (London) **225**, 535 (1970).

[4] A. M. Zhabotinsky, *Concentrations Autooscillations* (Nauka, Moscow, 1974) (in Russian).

[5] A.T. Winfree, Science **175**, 634 (1972).

[6] A.T. Winfree, *The Geometry of Biological Time* (Springer-Verlag, New York, 1980).

[7] *Oscillations and Traveling Waves in Chemical Systems*, edited by R. J. Field and M. Burger (Wiley, New York, 1985).

[8] Q. Quyang, V. Castets, J. Boissonade, J.C. Roux, P. De Kepper, and H.L. Swinney, J. Chem. Phys. **95**, 351 (1991).

[9] Z. Noszticius, W. Horsthemke, W.D. McCormick, and H.L. Swinney, Nature (London) **329**, 6140 (1987).

[10] P. De Kepper, I.R. Epstein, K. Kustin, and M. Orban, J. Phys. Chem. **86**, 170 (1982).

[11] E.C. Edblom, M. Orban, and I.R. Epstein, J. Am. Chem. Soc. **108**, 2826 (1986).

[12] V. Castets, E. Dulos, J. Boissonade, and P. De Kepper, Phys. Rev. Lett. **64**, 2953 (1990).

[13] P. De Kepper, V. Castets, E. Dulos, and J. Boissonade, Physica D **49**, 161 (1991).

[14] Q. Quyang and H.L. Swinney, Nature (London) **352**, 610 (1991).

[15] I. Lengyel, S. Kadar, and I.R. Epstein, Phys. Rev. Lett. **69**, 2729 (1992).

[16] E. Dulos, P. Davies, B. Rudovics, and P. De Kepper, Physica D **98**, 9 (1996).

[17] O. Steinbock, P. Kettunen, and K. Showalter, J. Phys. Chem. **100**, 18 970 (1996).

[18] W.Y. Tam, W. Horsthemke, Z. Noszticzius, and H.L. Swinney, J. Chem. Phys. **88**, 3395 (1988).

[19] G.S. Skinner and H.L. Swinney, Physica D **48**, 1 (1991).

[20] K.J. Lee, W.D. McCormick, Z. Noszticzius, and H.L. Swinney, J. Chem. Phys. **96**, 4048 (1992).

[21] Z. Noszticzius, Q. Quyang, W.D. McCormick, and H.L. Swinney, J. Phys. Chem. **96**, 6302 (1992).

[22] I. Lengyel and I.R. Epstein, Science **251**, 650 (1991).

[23] *Chemical Waves and Patterns*, edited by R. Kapral and K. Showalter (Kluwer, Dordrecht, 1995).

[24] K.J. Lee and H.L. Swinney, Phys. Rev. E **51**, 1899 (1995).

[25] G. Li, Q. Quyang, and H.L. Swinney, J. Chem. Phys. **105**, 10 830 (1996).

[26] J.J. Perraud, K. Agladze, E. Dulos, and P. De Kepper, Physica A **188**, 1 (1992).

[27] J.J. Perraud, A. De Wit, E. Dulos, P. De Kepper, G. Dewel, and P. Borckmans, Phys. Rev. Lett. **71**, 1272 (1993).

[28] P. De Kepper, J.J. Perraud, D. Rudovics, and E. Dulos, Int. J. Bifurcation Chaos Appl. Sci. Eng. **4**, 1215 (1994).

[29] G. Dewel, P. Borckmans, and A. De Wit, in *Far-from-*

Equilibrium Dynamics of Chemical Systems, edited by J. Gorecki, A.S. Cukrowski, A.L. Kawczyński, and B. Nowakowski (World Scientific, Singapore, 1994).
[30] P. Coullet, J. Lega, B. Houchmanzadeh, and J. Lajzerowicz, Phys. Rev. Lett. **65**, 1352 (1990).
[31] A. Hagberg and E. Meron, Phys. Rev. E **48**, 705 (1993).
[32] A. Hagberg and E. Meron, Phys. Rev. Lett. **72**, 2494 (1994).
[33] A. Hagberg and E. Meron, Chaos **4**, 477 (1994).
[34] C. Elphick, A. Hagberg, and E. Meron, Phys. Rev. E **51**, 3052 (1995).
[35] A. Hagberg, E. Meron, I. Rubinstein, and B. Zaltzman, Phys. Rev. Lett. **76**, 427 (1996).
[36] Ya.I. Kanel, Mat. Sb. **65**, 245 (1962).
[37] P. Fife, *Mathematical Aspects of Reacting and Diffusing Systems* (Springer-Verlag, Berlin, 1979).
[38] R.A. Fisher, Ann. Eugenics **7**, 355 (1937).
[39] A.N. Kolgomorov, I.G. Petrovsky, and N.S. Piskunov, Bjul. Moscovskovo. Gos. Univ. **17**, 1 (1937).
[40] A.N. Zaikin and A.L. Kawczyński, J. Non-Equilib. Thermodyn. **2**, 39 (1977).
[41] A.L. Kawczyński, Pol. J. Chem. **60**, 223 (1986).
[42] A.L. Kawczyński and A.N. Zaikin, J. Non-Equilib. Thermodyn. **2**, 139 (1977).
[43] J. Gorski and A.L. Kawczyński, Pol. J. Chem. **58**, 847 (1984).
[44] J. Gorski and A.L. Kawczyński, Pol. J. Chem. **59**, 61 (1985).
[45] A.L. Kawczyński, W.S. Comstock, and R.J. Field, Physica D **54**, 220 (1992).
[46] A.L. Kawczyński, J. Non-Equilib. Thermodyn. **3**, 29 (1979).
[47] A.L. Kawczyński, Pol. J. Chem. **57**, 1323 (1983).
[48] A.L. Kawczyński, Pol. J. Chem. **63**, 611 (1989).
[49] A.L. Kawczyński, Pol. J. Chem. **65**, 1759 (1991).
[50] B.S. Keener and V.V. Osipov, Sov. Phys. Usp. **32**, 101 (1989).
[51] B.S. Keener and V.V. Osipov, Sov. Phys. Usp. **33**, 679 (1990).
[52] C.B. Muratov and V.V. Osipov, Phys. Rev. E **53**, 3101 (1996).
[53] C.B. Muratov and V.V. Osipov, Phys. Rev. E **54**, 4860 (1996).
[54] J.E. Pearson, Science **261**, 189 (1993).
[55] V. Petrov, S.K. Scott, and K. Showalter, Philos. Trans. R. Soc. London, Ser. A **347**, 631 (1994).
[56] P. Gray and S.K. Scott, Chem. Eng. Sci. **39**, 1087 (1984).
[57] S.K. Scott, *Oscillations, Waves and Chaos in Chemical Kinetics* (Oxford University Press, Oxford, 1994).
[58] A.N. Tikhonov, Mat. Sb. **31**, 575 (1952).
[59] V.I. Arnold, *Ordinary Differential Equations* (Nauka, Moscow, 1984) (in Russian).
[60] A.L. Kawczyński, *Chemical Reactions from Equilibrium through Dissipative Structures to Chaos* (WN-T, Warsaw, 1990) (in Polish).
[61] J.D. Dockery and R.J. Field, Phys. Rev. E **58**, 823 (1998).
[62] J.A. Vastano, J.E. Pearson, W. Horsthemke, and H.L. Swinney, J. Chem. Phys. **88**, 6175 (1988).
[63] G. Dewel, A. DeWit, S. Metens, J. Verdasca, and P. Borckmans, Phys. Scr., T **T67**, 51 (1996).
[64] M. Bachir, P. Borckmans, and G. Dewel, Phys. Rev. E **59**, R6223 (1999).
[65] *Nonlinear Dynamics and Pattern Formation in Semiconductors and Devices*, edited by F.J. Niedernostheide (Springer-Verlag, Berlin, 1994).
[66] M. Gorman, M. el Hamdi, and K.A. Robbins, Combust. Sci. Technol. **98**, 37 (1994).
[67] M. Gorman, M. el Hamdi, and K.A. Robbins, Combust. Sci. Technol. **98**, 71 (1994).
[68] M. Gorman, M. el Hamdi, and K.A. Robbins, Combust. Sci. Technol. **98**, 79 (1994).
[69] J.D. Murray, *Mathematical Biology* (Springer-Verlag, New York, 1989).